Supporting Information

Tailoring Atomically Dispersed Cobalt-Nitrogen Active Sites in Wrinkled Carbon Nanosheets via "Fence" Isolation for Highly Sensitive Detection of Hydrogen Peroxide

Yue Hu[a], Chen Bai[b], Meng Li [a], Mirabbos Hojamberdiev[c], and Dongsheng Geng[a,d,*], Xiaoguang Li[e,*]

[a]*Beijing Advanced Innovation Center for Materials Genome Engineering, Beijing Key Laboratory for Magneto-Photoelectrical Composite and Interface Science, School of Mathematics and Physics, University of Science and Technology Beijing, Beijing 100083, China*

[b]*Tsinghua Shenzhen International Graduate School, Tsinghua University, Shenzhen 518055, China*

[c]*Institut für Chemie, Technische Universität Berlin, Straße des 17. Juni 135, 10623 Berlin, Germany*

[d]*School of Materials Science and Engineering, University of Science and Technology Beijing, Beijing 100083, China*

[e]*Institute of Intelligent Unmanned Systems, School of Automation, Qingdao University, Qingdao, 266071, China*

*Corresponding author: dgeng@ustb.edu.cn

lixiaoguang@qdu.edu.cn

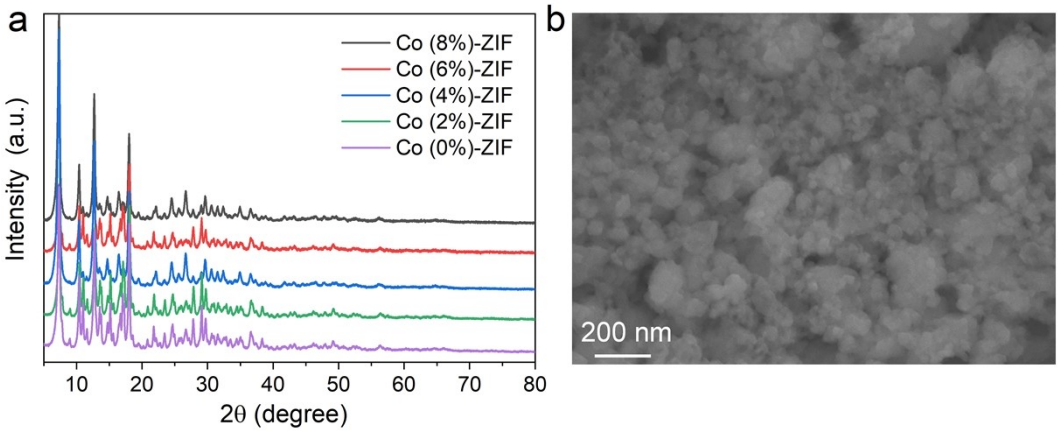

Figure S1. (a) XRD patterns of Zn/Co bimetallic ZIFs with different Zn/Co molar ratios (0, 2, 4, 6, and 8%) and (b) SEM image of Zn/Co ZIF (4% Co).

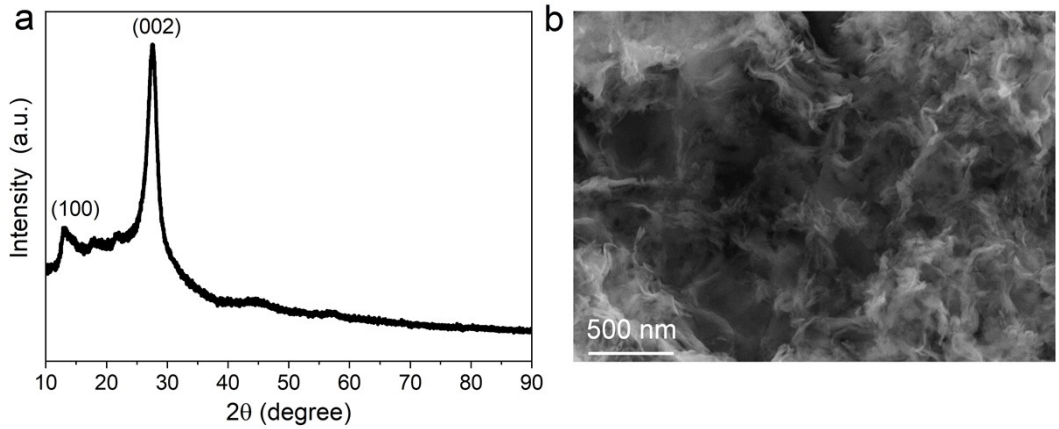

Figure S2. (a) XRD pattern and (b) SEM image of pristine g-C_3N_4.

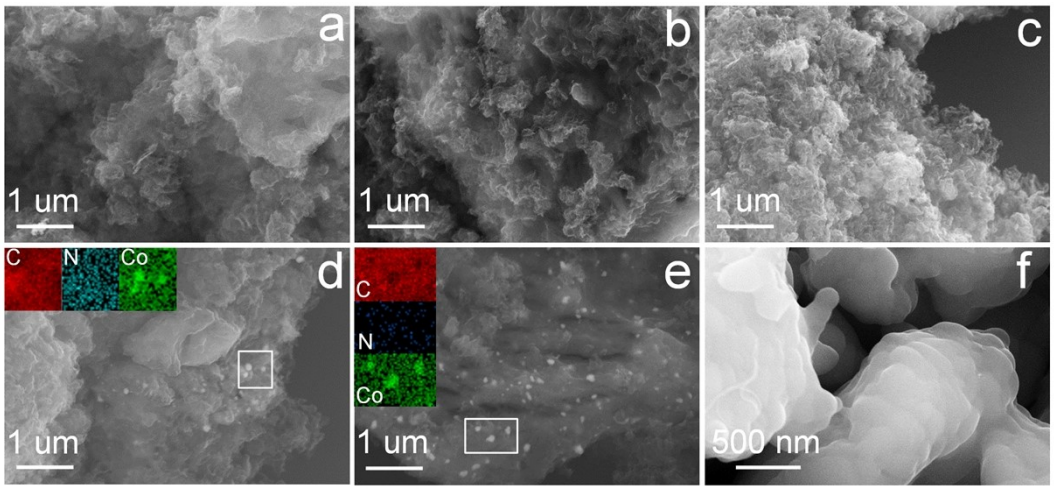

Figure S3. (a-e) SEM images of Co-N/CNS electrocatalysts obtained using g-C_3N_4 and Zn/Co ZIFs with different Zn/Co molar ratios and (f) SEM image of Co-N/C electrocatalyst obtained from Zn/Co ZIF (4% Co).

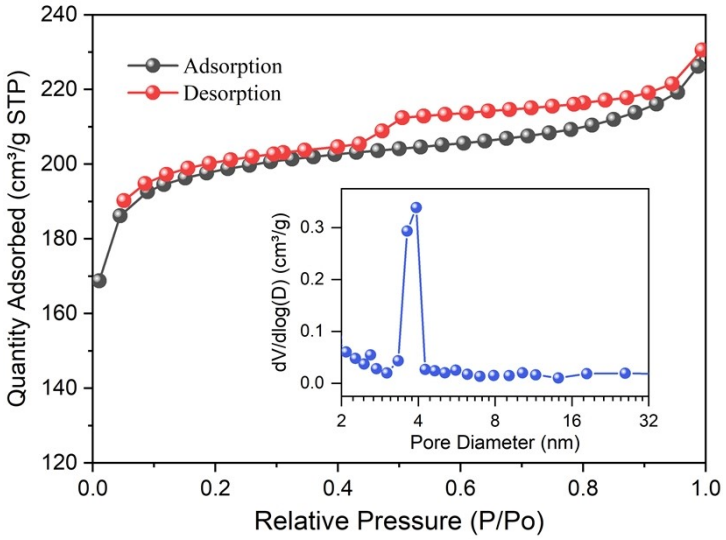

Figure S4. N_2 adsorption-desorption isotherm and pore-size distribution curve (inset) of Co (4%)-N/C.

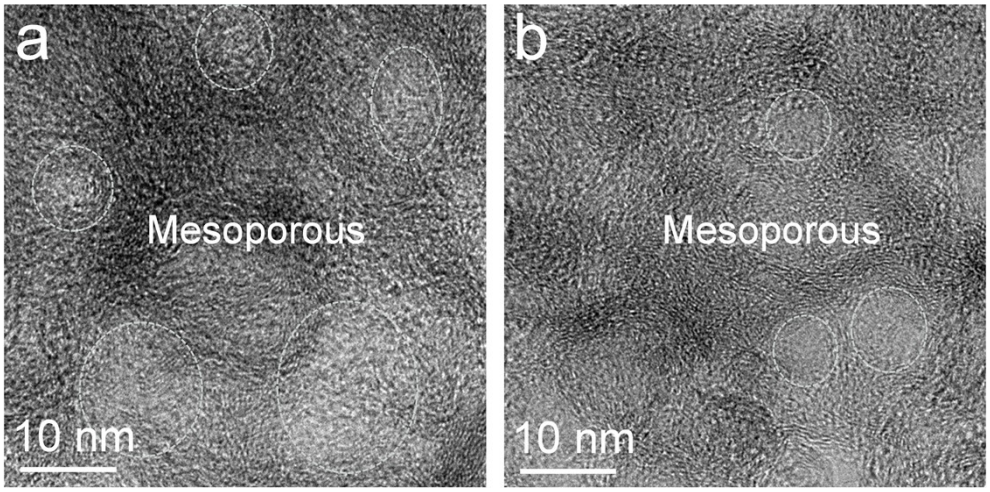

Figure S5. HRTEM images of Co (4%)-N/CNS. The white circles indicate mesopores.

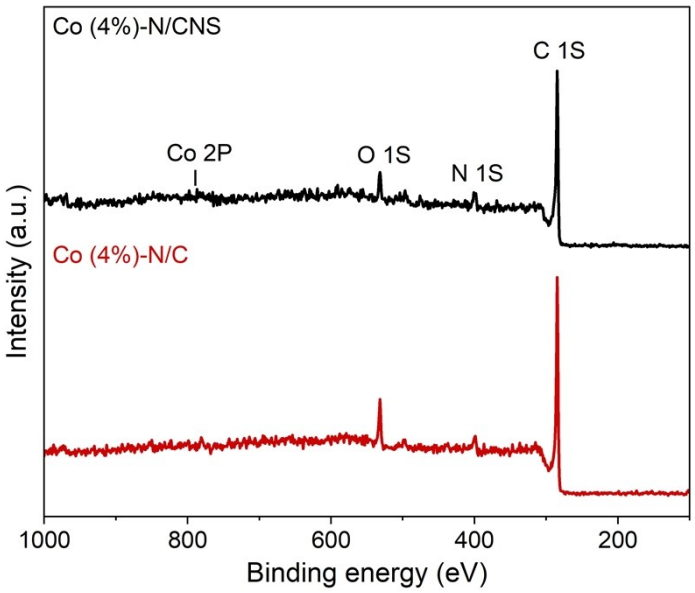

Figure S6. XPS survey spectra of Co (4%)-N/CNS and Co (4%)-N/C.

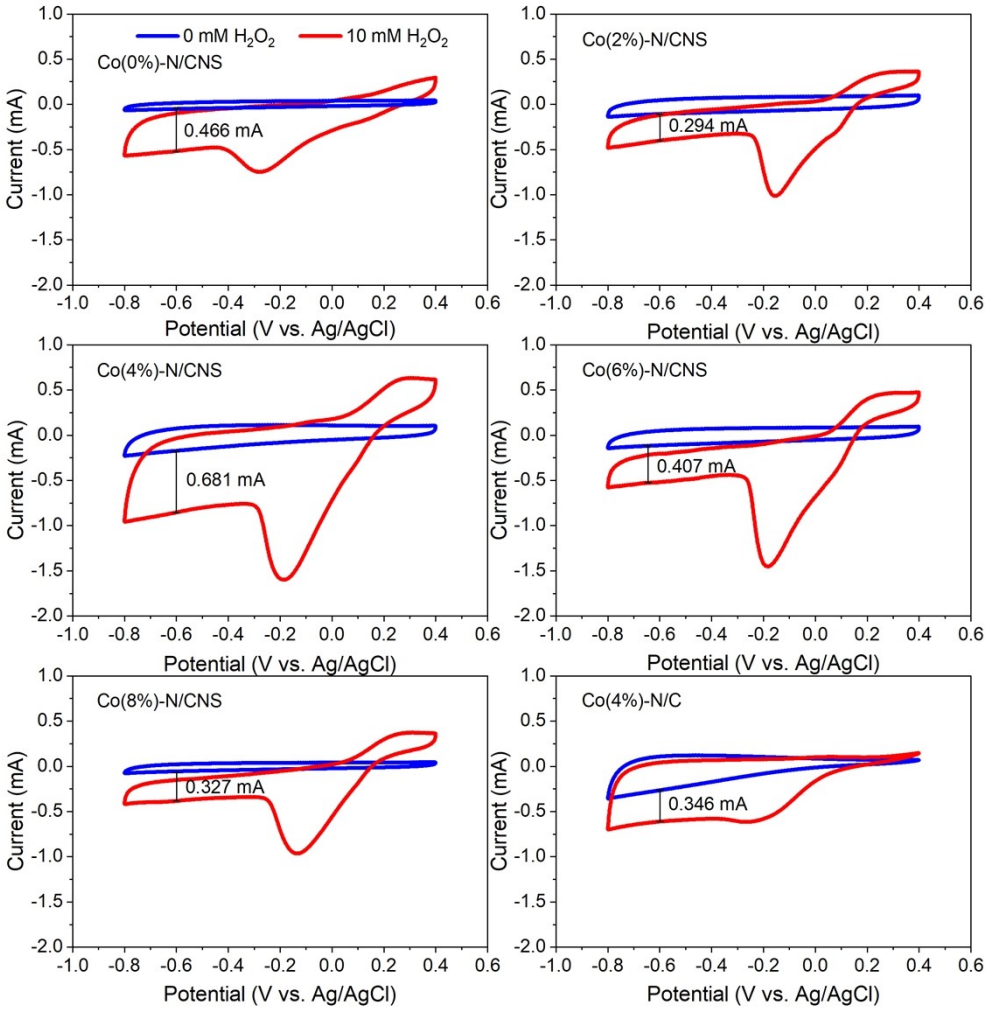

Figure S7. Catalytic reduction performance of Co (0%)-N/CNS, Co (2%)-N/CNS, Co (4%)-N/CNS, Co (6%)-N/CNS, Co (8%)-N/CNS, and Co (4%)-N/C toward 10 mM H_2O_2.

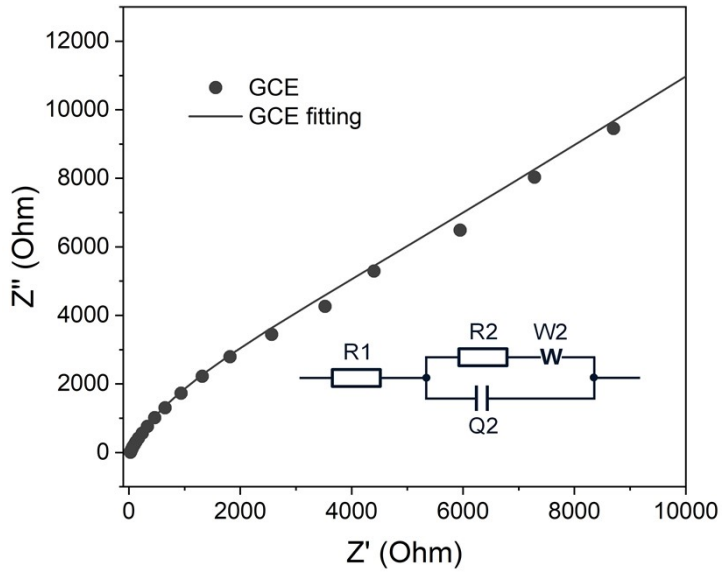

Figure S8. Nyquist plots measured at an applied potential of -0.7 V and corresponding equivalent circuit of bare GCE.

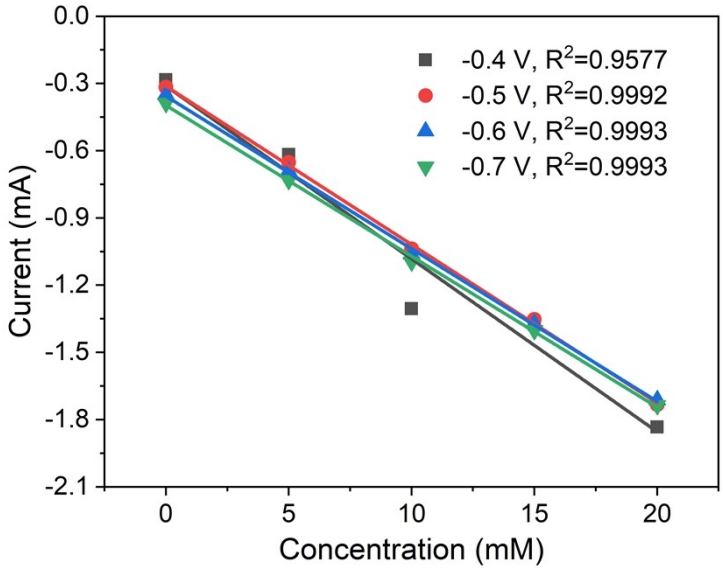

Figure S9. Reduction current responses of Co (4%)-N/CNS to different concentrations of H_2O_2 (0, 5, 10, and 20 mM) at different voltages (-0.4, -0.5, -0.6, and -0.7 V vs. Ag/AgCl).

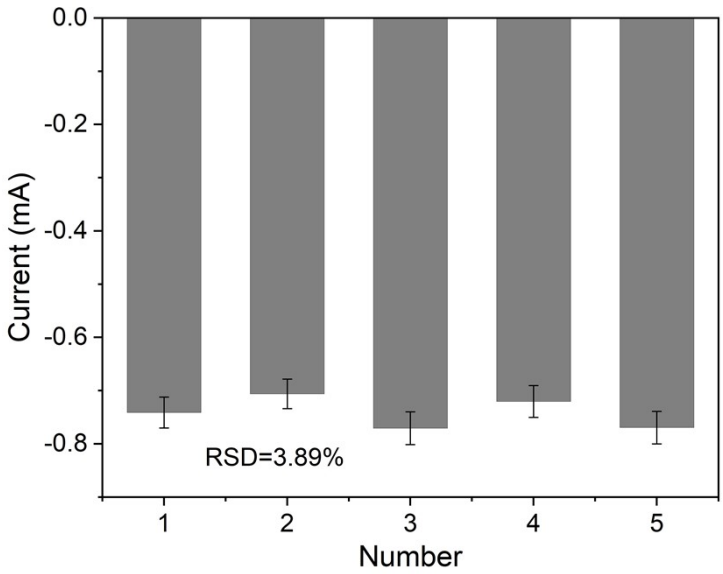

Figure S10. Current responses of Co (4%)-N/CNS-based sensors to 5 mM H_2O_2 in five consecutive cycles.

Table S1. Porous properties of Co (4%)-N/C and Co (4%)-N/CNS.

Materials	Porosity parameter				
	S_{BET} ($m^2 \cdot g^{-1}$)	V_t ($cm^3 \cdot g^{-1}$)	V_{mic} ($cm^3 \cdot g^{-1}$)	V_{mic}/V_t (%)	Average pore diameter (nm)
Co (4%)-N/C	767.54	0.34	0.27	79.41	4.43
Co (4%)-N/CNS	494.64	1.00	0.08	8.35	13.32

t – total and *mic* - micropore.

Table S2. Summary and comparison of mesoporosity and S_{BET} surface area of recently reported carbon catalysts derived from MOFs and/or g-C_3N_4.

Catalysts	Isotherm type	Mesopores (nm)	S_{BET} surface area ($m^2 \cdot g^{-1}$)	Reference
NHCS	II	2–25	122.73	[1]
N-FLG	IV	< 10	81.58	[2]
Co/N-BCNTs	IV	3–5	359	[3]
BCNT/Co	IV	< 10	291.4	[4]
Co-N/CNT	IV	2–4	261	[5]
CoP/NCNHP	IV	< 10	86.5	[6]
NCNTs-20	IV	–	151	[7]
N-Co/CNF-800	IV	2–6	223.89	[8]
NiCo-NC	IV	< 5	337.1	[9]
GCNs	IV	2–35~	377	[10]
Co (4%)-N/CNS	IV	2–50	494.6	This work

NHCS - nitrogen-doped hollow carbon spheres; FLG - few-layer graphene; BCNTs - bamboo-like carbon nanotube; CNTs – carbon nanotubes; NCNHP - N-doped carbon nanotube hollow polyhedron; CNF - carbon nanofibers; NC – nanocarbon; GCNs - graphitic carbon networks.

Table S3. Elemental content and percentage of C, N and Co of Co (4%)-N/C and Co (4%)-N/CNS (estimated by XPS analysis).

	Species	Co (4%)-N/C	Co (4%)-N/CNS
Elemental composition (wt%)	C 1s	81.26	82.31
	N 1s	7.25	8.64
	O 1s	9.16	7.57
	Co 2p	2.33	1.48
C (wt%)	C–C/C=C	54.46	55.73
	C–N	1.81	5.26
	C–O–C	5.14	4.53
	C=O	19.85	16.79
N (wt%)	Pyridinic N	0.96	1.68
	$Co–N_x$	1.01	2.04
	Pyrrolic N	0.68	1.5
	Graphite N	1.71	1.40
	Oxidized N	1.49	1.48
	Chemisorbed N	1.41	0.97
Co (wt%)	Co (II)	1.25	0.70
	$Co–N_x$	0.50	0.48

Table S4. Analytical performance of the ZIF-derived Co-N/C electrocatalysts-based non-enzymatic electrochemical H_2O_2 sensors.

Electrocatalysts	pH	Potential (V)	Linearity (μM)	LOD (μM)	Sensitivity ($\mu A \cdot mM^{-1} \cdot cm^{-2}$)	Response (s)	Reference
Co-N/C@G-B	–	0[a]	0.5–60000	0.19	2890	3	[11]
Co-NC RDCs	7.4	-0.3[b]	1–30000	0.143	234.913	<6	[12]
Co-N/CNT	7.0	-0.7[b]	0.05–50000	0.032	568.47	2–4	[5]
Co-NC/CNF	–	-0.5[b]	10–5000	10	300	–	[13]
Co (4%)-N/CNSs	7.0	-0.7[b]	1–500 500–1000000	0.006	468.95 605.50	<4	This work

[a]Reversible hydrogen electrode; [b]Ag/AgCl (in saturated KCl) electrode.

Table S5. Detection of H_2O_2 in real biological environment.

Sample	Added (μM)	Found[a] (μM)	RSD (%)	Recovery (%)
Serum 1	50	48.83	5.12	97.66
Serum 2	200	204.43	3.62	102.22

[a]Average of five determinations.

References

1. Y. H. Tang, X. Wang, J. J. Chen, X. X. Wang, D. J. Wang and Z. Y. Mao, *Carbon*, 2020, **168**, 458-467.
2. J. L. Liu, Y. Q. Zhang, L. Zhang, F. X. Xie, A. Vasileff and S. Z. Qiao, *Adv. Mater.*, 2019, **31**, 10.
3. R. Wang, T. Yan, L. Han, G. Chen, H. Li, J. Zhang, L. Shi and D. Zhang, *J. Mater. Chem. A*, 2018, **6**, 5752-5761.
4. X. J. Liu, W. X. Yang, L. L. Chen, Z. J. Liu, L. Long, S. Y. Wang, C. Y. Liu, S. J. Dong and J. B. Jia, *ACS Appl. Mater. Interfaces*, 2020, **12**, 4463-4472.
5. Z. Li, R. Liu, C. Tang, Z. Wang, X. Chen, Y. Jiang, C. Wang, Y. Yuan, W. Wang, D. Wang, S. Chen, X. Zhang, Q. Zhang and J. Jiang, *Small*, 2020, **16**, 1902860.
6. Y. Pan, K. A. Sun, S. J. Liu, X. Cao, K. L. Wu, W. C. Cheong, Z. Chen, Y. Wang, Y. Li, Y. Q. Liu, D. S. Wang, Q. Peng, C. Chen and Y. D. Li, *J. Am. Chem. Soc.*, 2018, **140**, 2610-2618.
7. P. P. Su, H. Xiao, J. Zhao, Y. Yao, Z. G. Shao, C. Li and Q. H. Yang, *Chem. Sci.*, 2013, **4**, 2941-2946.
8. Y. Wu, G. L. Xu, W. L. Zhang, C. Song, L. J. Wang, X. Y. Fang, L. J. Xu, S. G. Han, J. Q. Cui and L. Gan, *Carbohydr. Polym.*, 2021, **267**, 7.
9. L. Q. Zhao, Q. H. Wei, L. L. Zhang, Y. F. Zhao and B. Zhang, *Renewable Energy*, 2021, **173**, 273-282.
10. W. Zhang, X. Jiang, X. Wang, Y. V. Kaneti, Y. Chen, J. Liu, J.-S. Jiang, Y. Yamauchi and M. Hu, *Angew. Chem.*, 2017, **56**, 8435-8440.
11. Z. Li, W. Wang, H. Cao, Q. Zhang, X. Zhou, D. Wang, Y. Wang, S. Zhang, G. Zhang, C. Liu, Y. Zhang, R. Liu and J. Jiang, *Adv. Mater. Technol.*, 2017, **2**, 1700224.
12. Z. Wu, L.-P. Sun, Z. Zhou, Q. Li, L.-H. Huo and H. Zhao, *Sens. Actuators, B*, 2018, **276**, 142-149.
13. M. A. Riaz, Z. Yuan, A. Mahmood, F. Liu, X. Sui, J. Chen, Q. Huang, X. Liao, L. Wei and Y. Chen, *Sens. Actuators, B*, 2020, **319**, 128243.